

Development of a 2.0 eV AlGaInP Solar Cell Grown by OMVPE

Emmett E. Perl^{1,2}, John Simon¹, John F. Geisz¹, Waldo Olavarria¹, Michelle Young¹, Anna Duda¹, Pat Dippo¹, Daniel J. Friedman¹ and Myles A. Steiner¹

¹National Renewable Energy Laboratory, Golden, CO, 80401, USA

²University of California at Santa Barbara, Santa Barbara, CA, 93106, USA

Abstract — AlGaInP solar cells with a bandgap (E_g) of ~ 2.0 eV are developed for use in next-generation multijunction photovoltaic devices. This material system is of great interest for both space and concentrator photovoltaics due to its high bandgap, which enables the development of high-efficiency five-junction and six-junction devices and is also useful for solar cells operated at elevated temperatures. In this work, we explore the conditions for the Organometallic Vapor Phase Epitaxy (OMVPE) growth of AlGaInP and study their effects on cell performance. A ~ 2.0 eV AlGaInP solar cell is demonstrated with an open circuit voltage (V_{OC}) of 1.59V, a bandgap-voltage offset (W_{OC}) of 420mV, a fill factor (FF) of 88.0%, and an efficiency of 14.8%. These AlGaInP cells have attained a similar FF, W_{OC} and internal quantum efficiency (IQE) to the best upright GaInP cells grown in our lab to date.

Index Terms — III-V semiconductor materials, photovoltaic cells, semiconductor epitaxial layers, solar energy.

I. INTRODUCTION

Multijunction solar cells have long achieved the highest efficiencies of any photovoltaic technology. Today, the world's best devices consist of four or more III-V semiconductor junctions and have attained power conversion efficiencies greater than 38% at one-sun and 45% under concentration [1]. To achieve these high efficiencies, each of the subcells needs to meet a few key requirements. First, they must have a bandgap (E_g) that is close to the optimal in order to minimize the combined thermalization and non-absorption loss in the final structure [2-5]. Second, they must be composed of excellent quality materials with effective passivation layers in order to avoid substantial losses to the open circuit voltage (V_{OC}) and short circuit current density (J_{SC}). Today's best four-junction devices have demonstrated a bandgap-voltage offset ($W_{OC} = E_g/q - V_{OC}$) ≤ 400 mV for each subcell when illuminated at one-sun, which is indicative of the excellent material quality of these devices [6,7]. Third, if a monolithic two-terminal configuration is desired, the subcells must be integrated together. This requires proper optical design and the development of a tunnel junction between each subcell [2,8,9]. Even though lattice-matching constraints make it difficult to grow each subcell on the same substrate, the most efficient multijunction solar cells reported to date have been successfully integrated into monolithic two-terminal devices using either semiconductor bonding or lattice-mismatched growth techniques [6,7,10].

While four-junction photovoltaic devices have attained great success in recent years, the field is rapidly moving toward designs with five or six semiconductor junctions to

further increase efficiencies [10,11]. Recently, Chiu *et al.* reported a five-junction device with a one-sun world record efficiency of 38.8%, albeit with a higher average W_{OC} of 440mV for the top three subcells [1,10]. This suggests that improvements to the material quality of these subcells could pave the way to even higher efficiencies. While the ternary alloy GaInP can be grown with excellent material quality and a near-optimal bandgap for a four-junction device, higher quality top cells with larger bandgap energies are desired for five-junction and six-junction photovoltaic devices [4,5,12].

Higher bandgaps are also preferred for photovoltaic devices that are operated at elevated temperatures. Landis *et al.* reported on the development of high-temperature solar cells for near-sun space missions, and show how the optimal room-temperature (RT) bandgap of a single-junction solar cell shifts from around 1.4 eV for operation at 25°C to 2.3 eV for operation at 900°C [13].

We are interested in developing a two-junction photovoltaic device that can operate efficiently at temperatures up to 400°C for use in hybrid Concentrator Photovoltaic/Concentrator Solar Power (CPV/CSP) systems. Fig. 1 shows the modeled efficiency for a two-junction device as a function of operating temperature and the RT bandgap of the top cell. This model constrains the RT bandgap of the bottom subcell to 1.42 eV (GaAs) and assumes a concentration of 1000 suns, a one-sun W_{OC} of 400mV for each subcell at RT, and that all absorbed photons are converted into photocurrent.

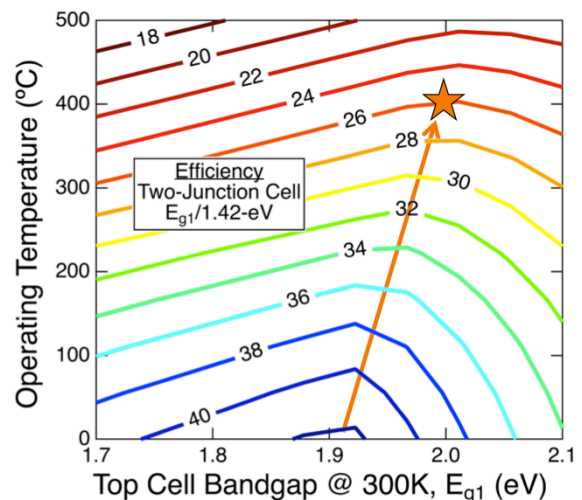


Fig. 1. Modeled efficiency of a two-junction photovoltaic device as a function of the top cell's room-temperature (300K) bandgap and the operating temperature.

The key takeaways from this plot are that the ideal RT bandgap of the top cell increases and that the cell efficiency decreases as the operating temperature is increased. A two-junction device with subcell bandgaps of 2.0 eV and 1.42 eV is near optimal for a device operated at 400°C, and can theoretically reach an efficiency greater than 25%.

The quaternary alloy AlGaInP offers the highest direct bandgap of any III-V material that is lattice-matched to GaAs. It is therefore a promising candidate for use in five-junction and six-junction photovoltaic devices as well as for solar cells operated at high temperature. By increasing the aluminum content of the alloy from 0% to approximately 25%, direct bandgaps between 1.9 eV and 2.26 eV are achievable [14,15].

While AlGaInP has great potential for improving the efficiency of the next-generation of multijunction devices, there are several technical challenges that accompany its development. Chief among these is the issue of oxygen contamination, which can be problematic for any aluminum-containing material due to the high dissociation energy of the bond between aluminum and oxygen [14,16]. The incorporation of oxygen is often associated with the formation of deep-level traps that can greatly increase the non-radiative recombination rate of a material [17].

Despite the growth challenges, a number of groups have worked to develop high-bandgap AlGaInP cells [18-20]. Masuda *et al.* reported a 2.0 eV AlGaInP subcell grown by molecular beam epitaxy (MBE) with a W_{OC} of 620mV, but with a lower internal quantum efficiency (IQE) than that of a GaInP cell [18]. Hongbo *et al.* demonstrated a 2.05 eV AlGaInP subcell grown by organometallic vapor phase epitaxy (OMVPE) with a W_{OC} of 595mV, but also observed degradation in the IQE [19]. Cornfeld *et al.* developed a 2.05 eV AlGaInP solar cell that achieved a W_{OC} of 510mV with significantly less degradation in the IQE [20]. No AlGaInP cell reported to date has achieved a comparable IQE and W_{OC} to that of the best GaInP subcells [12]. Reducing the W_{OC} to around 400mV while maintaining a high IQE is necessary to successfully integrate AlGaInP into a multijunction device.

In this work, we report on the development of a ~2.0 eV AlGaInP subcell. Under the direct spectrum at 1000W/m² (AM1.5D), the best of these samples had a V_{OC} of 1.59V, W_{OC} of 420mV, fill factor of 88.0%, and efficiency of 14.8%. Additionally, we note that we did not observe any degradation in the IQE of the AlGaInP cells compared to upright GaInP cells grown under similar conditions.

II. EXPERIMENTAL METHODS

All the samples in this study were grown using an atmospheric pressure OMVPE vertical reactor. The reactor is custom built and uses trimethylgallium (TMGa), triethylgallium (TEGa), trimethylindium (TMIn), trimethylaluminum (TMAI), arsine (AsH₃), and phosphine (PH₃) sources. Diethylzinc (DEZn) was added to p-dope the

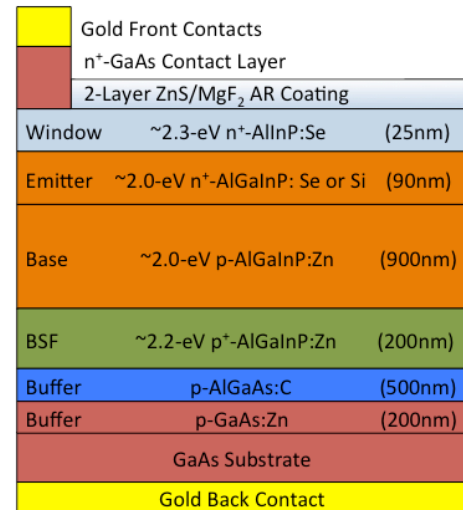


Fig. 2. Schematic of a 2.0 eV AlGaInP cell showing the structure of the epitaxially grown layers, antireflection (AR) coating, and metallization. The diagram is not to scale.

back surface field (BSF) and base layers, and either dilute hydrogen selenide (H₂Se/H₂) or disilane (Si₂H₆/H₂) was added to n-dope the emitter and window layers. Prior to growth, the GaAs substrates were etched for one minute in a NH₄OH:H₂O₂:H₂O (2:1:10) solution and a graphite susceptor at the center of the reactor was heated to a temperature of 1000°C to drive excess oxygen out of the reactor.

Fig. 2 shows a schematic of the device that includes the nominal bandgap and thickness of the semiconductor layers. A ~500nm AlGaAs buffer layer was grown prior to the active device layers in order to getter residual oxygen early in the growth. The active device consists of a ~200nm AlGaInP BSF with a nominal Al composition of 27%, a ~900nm AlGaInP base with a nominal Al composition of 12%, a ~90nm AlGaInP emitter with a nominal Al composition of 12%, and a ~25nm AlInP window layer. All of the active layers were grown at a rate > 6.5μm/hr and a phosphine overpressure (V/III ratio) > 400. The growth temperature (T_g) of these layers was varied from 700°C to 800°C. After growth, the cells were processed using standard photolithography and wet chemical etching techniques. Only the samples grown with varying T_g were antireflection (AR) coated.

After the AlGaInP cells were processed, we performed IQE measurements using a custom-built test setup to estimate the collection efficiency and bandgap of the devices. RT Hall and Capacitance-Voltage (CV) measurements were taken to estimate the concentrations of the p-type and n-type dopants. We also took illuminated current-voltage (LIV), dark current-voltage (DIV), and electroluminescence (EL) measurements for each device. These measurements were performed using a custom-built solar simulator, which is calibrated using reference cells to provide a one-sun illumination under the AM1.5D spectrum. These test setups are discussed in more detail elsewhere [2,6,12].

III. RESULTS AND DISCUSSION

A. Substrate Miscut

The bandgap of a given AlGaInP alloy has been shown to vary by around 100 meV depending on the degree of CuPt-type ordering [14,18,21,22]. To determine the effect of T_g and substrate miscut angle on ordering, we grew a set of AlGaInP layers on GaAs substrates that were miscut 2° toward the (111)A direction (2° A), 4° toward the (111)B direction (4° B), 6° toward the (111)A direction (6° A), and 6° toward the (111)B direction (6° B) and measured the resulting peak emission wavelength using RT photoluminescence (PL). These results are shown in Fig. 3.

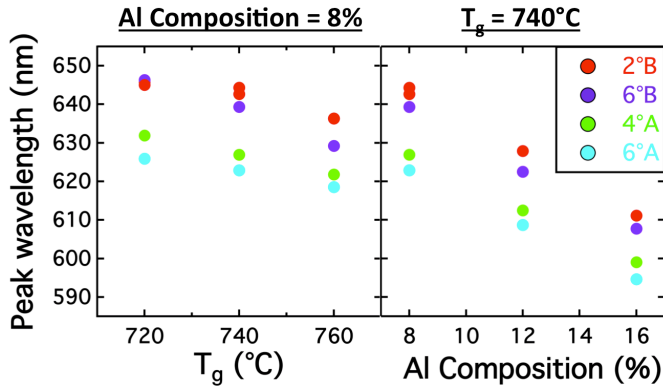


Fig. 3. Peak wavelength measured with RT PL as a function of (left) growth temperature and (right) aluminum composition for AlGaInP layers grown on 2° B, 4° A, 6° A, and 6° B GaAs substrates.

There are a few key takeaways from the PL results. First, increasing the aluminum content clearly raises the bandgap of the AlGaInP layers and therefore lowers the peak emission wavelength, as expected. Second, the 6° A substrates yield the lowest emission wavelengths of all the substrates considered with a peak emission wavelength that is about 20nm lower than for the 2° B substrates. Third, increasing the T_g appears to slightly decrease the peak emission wavelength, although only by about 5-10nm as the T_g is increased from 720°C to 760°C .

These shifts in the peak wavelength are likely caused by a change in the degree of ordering in the AlGaInP layers, due to both temperature and substrate miscut, which is consistent with trends reported in the literature for GaInP [18,21,22]. By growing more disordered AlGaInP, it is possible to achieve our target 2.0 eV bandgap with a lower aluminum composition than if we were to grow more ordered AlGaInP, helping to minimize oxygen contamination in the AlGaInP layers. All of the solar cells shown in the next sections are grown on 6° A GaAs substrates

B. Emitter Doping

The emitter doping can have a significant impact on device performance. The first samples that we grew used silicon as the n-type dopant in the AlGaInP emitter. While we were able

to obtain a fairly high V_{OC} from these samples, we measured a large decrease in the IQE at short wavelengths compared to GaInP cells grown under similar conditions. This reduction in the IQE of the emitter is similar to what has been seen in previous studies of AlGaInP solar cells [18-20].

We later grew samples using selenium as the n-type dopant, and consistently observed a full recovery in the IQE. Fig. 4 shows the IQE of AlGaInP solar cells, grown at 740°C , with silicon-doped and selenium-doped emitters. From RT Hall measurements, we found that the emitter dopant concentration in both of these samples is around $1 \times 10^{18} \text{ cm}^{-3}$.

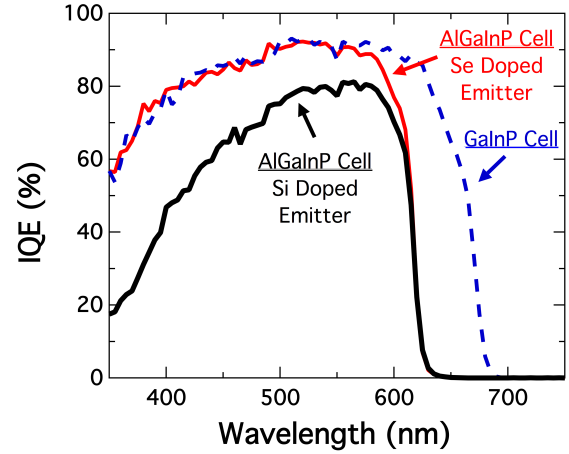


Fig. 4. IQE for AlGaInP solar cells with a silicon-doped (black) and selenium-doped (red) emitter. The dashed blue line shows the IQE for a GaInP solar cell grown under similar conditions.

By replacing silicon with selenium as the n-type dopant, we were able to achieve a comparable IQE to that of an upright GaInP cell for the strongly absorbed light above the bandgap of AlGaInP. These samples also had a notably higher J_{SC} and V_{OC} than the silicon-doped samples. Fig. 5 shows the I-V characteristics of both AlGaInP samples when illuminated under a simulated AM1.5D spectrum.

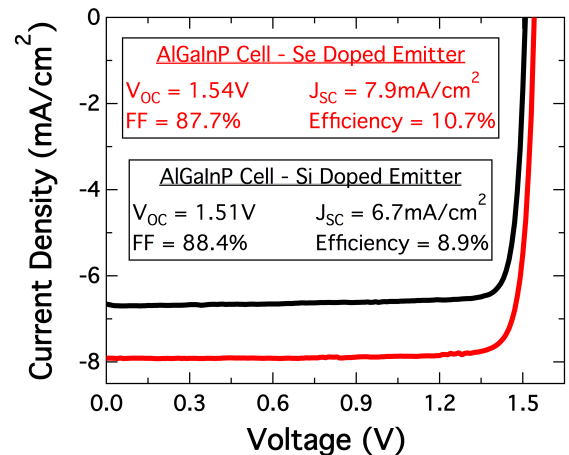


Fig. 5. One-sun LIV measurements for AlGaInP solar cells with a silicon-doped (black) and selenium-doped (red) emitter.

TABLE I
SOLAR CELL PARAMETERS FOR SAMPLES GROWN AT DIFFERENT TEMPERATURES

Sample	T_g (°C)	E_g (eV)	V_{oc} (V)	W_{oc} (mV)	η_{ext} @ one-sun (%)	J_{sc} (mA/cm ²)	FF (%)	Efficiency (%)
MN742	700	1.97	1.49	480	0.12	10.9	73.1	11.9
MN746	720	1.98	1.51	470	0.17	10.6	81.7	13.0
MN750	740	1.99	1.55	440	0.40	10.7	87.9	14.6
MN753	760	2.00	1.56	440	0.41	10.7	88.4	14.7
MN775	780	2.01	1.59	420	0.75	10.6	88.0	14.8
MN779	800	2.03	1.57	460	0.19	10.3	88.2	14.2

C. Growth Temperature

The material quality of OMVPE grown AlGaInP is very sensitive to T_g , which affects both oxygen incorporation and CuPt-type ordering [14]. To study the impact of T_g on cell performance, we grew a set of ~ 2.0 eV solar cells where we varied the T_g of the AlGaInP layers from 700°C to 800°C while keeping all other growth conditions the same. These samples had a 2-layer ZnS/MgF₂ AR Coating and used selenium as the n-type dopant for the emitter.

Table I shows the measured cell parameters for each of these devices. We found that cell performance improved as the T_g was increased up to 780°C. By increasing T_g from 700°C to 780°C, we were able to decrease the W_{oc} from 480mV to 420mV, increase the fill factor from 73.1% to 88.0%, and increase the efficiency from 11.9% to 14.8%.

This trend is not surprising. It is well known that high growth temperatures can suppress the incorporation of oxygen due to the increased probability of desorption from the surface. Minimizing oxygen contamination can help reduce the non-radiative recombination rate in the AlGaInP layers, which can significantly improve cell performance [14,16].

There are a number of other important trends that we observed. First, we found that the bandgap increases with T_g . This can be partially explained by a decrease in CuPt-type ordering with growth temperature. However, the higher bandgaps could also be a result of lower indium incorporation

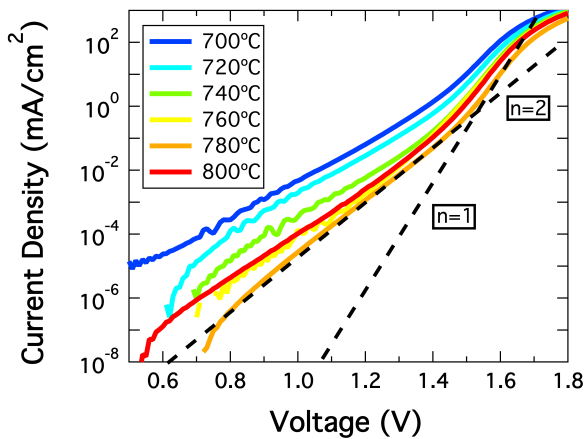


Fig. 6. Dark I-V measurements of AlGaInP solar cells grown at temperatures of 700°C to 800°C.

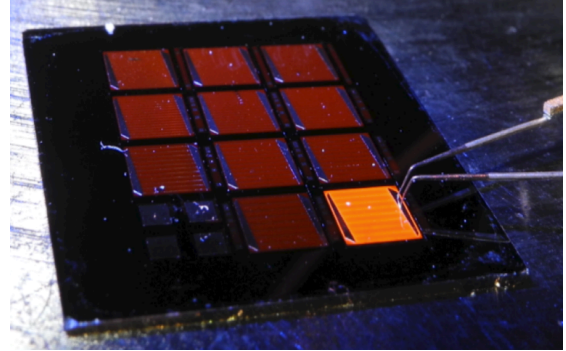


Fig. 7. Luminescence from the AlGaInP solar cell grown at 780°C. A blue LED is illuminating the sample, causing photoluminescence in the ten devices that appear red. Current is also injected across the device on the bottom right, causing it to luminesce brighter and appear orange.

at high T_g . Using an in-situ wafer curvature measurement technique (MOS) [23], we observed increased tensile strain for the samples grown at 780°C and 800°C, which is indicative of a lower indium composition and higher bandgap. This high strain could also explain why the performance of the sample grown at 800°C was degraded.

It is also important to stress that none of the OMVPE flow rates were changed as the T_g was varied. This resulted in lower concentrations of the zinc and selenium dopants for the samples grown at high temperatures. Like oxygen, both zinc and selenium incorporate less efficiently at high T_g .

While the doping concentration will certainly impact the I-V characteristics of a cell, we would expect a device with lower doping to have higher dark currents and therefore a lower V_{oc} [24]. We would also expect a device with lower doping to have a lower external radiative efficiency (η_{ext}) [25]. However, we observe the opposite trend up to a T_g of 780°C. This can be explained if the non-radiative recombination rate is lower for the samples grown at higher temperatures.

Fig. 6 shows the dark I-V characteristics for each of these cells. The dashed lines indicate the slopes of ideal diodes with ideality factors of 1 and 2 and y-intercepts equal to J_{01} for the $n=1$ line and J_{02} for the $n=2$ line. It is clear that both J_{01} and J_{02} are decreasing as the T_g is increased up to 780°C. These reduced dark currents are indicative of lower non-radiative recombination rates, which likely result from lower oxygen incorporation for the samples grown at high temperature.

A picture of the best sample, grown at 780°C, is shown in Fig. 7. These devices have a bandgap ~ 2.0 eV, which corresponds to orange emission. Current is injected across the device on the bottom right, causing it to luminesce bright orange. A blue LED is illuminating the entire sample, causing photoluminescence in the other ten devices. These devices appear red because the blue light from the LED is mixing with the less intense orange light emitted from these devices. These samples have a similar W_{OC} , FF, and IQE to the best upright GaInP cells grown at NREL to date [12].

D. Cell Thickness

Cell thickness can directly impact J_{SC} , which is important for current matching in a multijunction solar cell. If a subcell has excess photocurrent, it can be thinned in order to lower its J_{SC} by reducing its long wavelength IQE. On the other hand, if an optically thinned subcell is undersupplied with photocurrent, it can be thickened in order to raise its J_{SC} by increasing its long wavelength IQE. If, however, the thickness of the absorber exceeds the minority carrier diffusion length, it will not be possible to collect the carriers that were generated far from the junction and the long wavelength IQE can be degraded [26].

To study the impact of cell thickness on solar cell performance, we grew a set of four samples where we varied the nominal thickness of the base from 0.4 μm to 2.9 μm . These samples were grown at 780°C using selenium as the n-type dopant for the emitter. The total nominal thickness for these four cells was 0.5 μm , 1.0 μm , 2.0 μm , and 3.0 μm . The resulting IQE's for these devices are shown in Fig. 8.

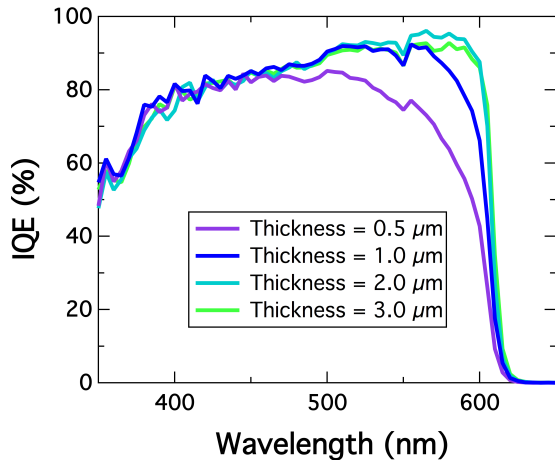


Fig. 8. IQE measurements of AlGaInP solar cells with thicknesses between 0.5 μm and 3.0 μm .

There is a clear improvement in the long wavelength IQE as the cell thickness is increased from 0.5 μm to 2.0 μm . This is because the 0.5- μm and 1.0- μm cells are not optically thick and only absorb a fraction of the long wavelength photons. As the cell thickness is increased from 2.0 μm to 3.0 μm , we

observe a minimal change in the IQE. This suggests that the 2.0- μm thick cell is very close to optically thick, and that there is little or no benefit to increasing the thickness further.

It is also important to note that we do not see significant degradation in the long wavelength IQE for the 3.0- μm thick cell. This suggests that even at 3.0 μm , it is possible to collect nearly all of the photogenerated carriers in the base.

IV. SUMMARY

In this work, we developed a 2.0 eV AlGaInP solar cell grown by OMVPE for use in the next-generation of multijunction photovoltaic devices. We explored the growth conditions for the AlGaInP layers, and found that the choice of emitter dopant, the growth temperature, and the cell thickness have a pronounced effect on cell performance.

Early attempts to grow cells with silicon-doped emitters yielded a V_{OC} around 1.51V, but with considerable degradation in the IQE for these devices. By switching to selenium as the n-type dopant, we were able to consistently recover the IQE and increase the V_{OC} by ~ 30 mV.

We then grew a set of samples where we varied the growth temperature from 700°C to 800°C, and found a strong correlation between T_g and device performance. By increasing the growth temperature from 700°C to 780°C, we were able to decrease the W_{OC} from 480mV to 420mV and increase the efficiency from 11.9% to 14.8%.

Finally, we grew a set of samples where we varied the nominal absorber thickness from 0.5 μm to 3.0 μm . By increasing the cell thickness from 0.5 μm to 2.0 μm , we were able to significantly increase long wavelength IQE and J_{SC} of the cell. However, there was little difference between the IQE of the 2.0 μm and the 3.0 μm cell, indicating that the 2.0 μm cell is very close to optically thick and that there is little benefit to further increasing the thickness.

These AlGaInP devices have attained a comparable W_{OC} , FF, and IQE to that of the best upright GaInP cells grown at NREL. The next step is to integrate these high-bandgap AlGaInP subcells into high-temperature dual-junction photovoltaic devices and into our future inverted metamorphic solar cells. The integration of AlGaInP into the next-generation of multijunction photovoltaic devices should enable solar cell efficiencies to reach new heights.

ACKNOWLEDGEMENTS

Research was supported by the U.S. Department of Energy under Contract no. DE-AC36-08GO28308 with the National Renewable Energy Laboratory (NREL) and funded in part by the ARPA-E FOCUS program award no. DE-AR0000508 (PI: Minjoo Lee, Yale University). The work by E. E. Perl was funded in part by the Alliance for Sustainable Energy, LLC, Managing and Operating Contractor for NREL for the U. S. Department of Energy.

REFERENCES

- [1] M. A. Green, K. Emery, Y. Hishikawa, W. Warta, and E. D. Dunlop, "Solar cell efficiency tables (version 45)", *Progress in Photovoltaics: Research and Applications*, vol. 23, no. 1, pp. 1-9, 2015.
- [2] D. J. Friedman, J. M. Olson, and S. R. Kurtz, *High-efficiency III-V multijunction solar cells, Handbook of photovoltaic science and engineering, 2nd ed.*, A. Luque and S. Hegedus, Ed. (Wiley, Chichester UK, 2011) pp. 314-364.
- [3] W. Shockley and H. J. Queisser, "Detailed balance limit of efficiency of p-n junction solar cells", *Journal of Applied Physics*, vol. 32, no. 3, pp. 510-519, 1961.
- [4] D. C. Law, R. R. King, E. Yoon, M. J. Archer, A. Boca, C. Fetzer, S. Mesropian, T. Isshiki, M. Haddad, K. M. Edmondson, D. Bhusari, J. T. Yen, R. A. Sherif, H. A. Atwater, and N. H. Karam, "Future technology pathways of terrestrial III-V multijunction solar cells for concentrator photovoltaic systems", *Solar Energy Materials and Solar Cells*, vol. 94, no. 8, pp. 1314-1318, 2010.
- [5] R. R. King, A. Boca, W. Hong, X.-Q. Liu, D. Bhusari, D. Larrabee, K. M. Edmondson, D. C. Law, C. M. Fetzer, S. Mesropian, and N. H. Karam, "Band-gap-engineered architectures for high-efficiency multijunction concentrator solar cells", in *24th European Photovoltaic Solar Energy Conference and Exhibition, 2009*,
- [6] R. M. France, J. F. Geisz, M. A. Steiner, I. Garcia, W. E. McMahon, and D. J. Friedman, "Quadruple junction inverted metamorphic concentrator devices", *IEEE Journal of Photovoltaics*, vol. 5, no. 1, pp. 432, 2015.
- [7] F. Dimroth, M. Grave, P. Beutel, U. Fiedeler, C. Karcher, T. N. D. Tibbits, E. Oliva, G. Siefer, M. Schaechtner, A. Wekkeli, A. W. Bett, R. Krause, M. Piccin, N. Blanc, C. Drazek, E. Guiot, B. Ghyselen, T. Salvetat, A. Tauzin, T. Signamarcheix, A. Dobrich, T. Hannappel, and K. Schwarzburg, "Wafer bonded four-junction GaInP/GaAs/GaInAsP/GaInAs concentrator solar cells with 44.7% efficiency", *Progress in Photovoltaics: Research and Applications*, vol. 22, no. 3, pp. 277-282, 2014.
- [8] E. E. Perl, W. E. McMahon, R. M. Farrell, S. P. DenBaars, J. S. Speck, and J. E. Bowers, "Surface structured optical coatings with near-perfect broadband and wide-angle antireflective properties", *Nano Letters*, vol. 14, no. 10, pp. 5960-5964, 2014.
- [9] E. E. Perl, W. E. McMahon, D. J. Friedman, and J. E. Bowers, "Design of antireflective nanostructures and optical coatings for next-generation multijunction photovoltaic devices", *Optics Express*, vol. 22, no. S5, pp. A1243-A1256, 2014.
- [10] P. T. Chiu, D. C. Law, R. L. Woo, S. B. Singer, D. Bhusari, W. D. Wong, A. Zakaria, J. Boisvert, S. Mesropian, R. R. King, and N. H. Karam, "Direct semiconductor bonded 5J cell for space and terrestrial applications", *IEEE Journal of Photovoltaics*, vol. 4, no. 1, pp. 493, 2014.
- [11] P. Patel, D. Aiken, D. Chumney, A. Cornfeld, Y. Lin, C. Mackos, J. McCarty, N. Miller, P. Sharps, and M. Stan, "Initial results of the monolithically grown six-junction inverted metamorphic multi-junction solar cell", in *38th IEEE Photovoltaic Specialist Conference, 2012*, pp. 1-4.
- [12] J. F. Geisz, M. A. Steiner, I. Garcia, S. R. Kurtz, and D. J. Friedman, "Enhanced external radiative efficiency for 20.8% efficient single-junction GaInP solar cells", *Applied Physics Letters*, vol. 103, no. 4, pp. 041118, 2013.
- [13] G. A. Landis, D. Merritt, R. Raffaele, and D. Scheiman, "High-temperature solar cell development", in *18th Space Photovoltaic Research and Technology Conference, 2005*, pp. 241-247.
- [14] *High brightness light emitting diodes, Semiconductors and semimetals*, G. B. Stringfellow and M. G. Craford, Ed. (Academic Press, 1997), vol. 48.
- [15] Y.-G. Zhan and Y. Gu, *Al(Ga)InP-GaAs photodiodes tailored for specific wavelength range, Photodiodes - from fundamentals to applications*, I. Yun, Ed. (INTECH Open Access Publisher, 2012).
- [16] G. B. Stringfellow, *Organometallic vapor-phase epitaxy: Theory and practice* (Academic Press, 1999).
- [17] S. Heckelmann, D. Lackner, C. Karcher, F. Dimroth, and A. W. Bett, "Investigations on AlGaAs solar cells grown by MOVPE", *IEEE Journal of Photovoltaics*, vol. 5, no. 1, pp. 446-453, 2014.
- [18] T. Masuda, S. Tomasulo, J. R. Lang, and M. L. Lee, "Comparison of single junction AlGaInP and GaInP solar cells grown by molecular beam epitaxy", *Journal of Applied Physics*, vol. 117, no. 9, pp. 094504, 2015.
- [19] L. Hongbo, L. Xinyi, Z. Wei, Z. Dayong, S. Mengqui, S. Lijie, and C. Kaijian, "A 2.05 eV AlGaInP sub-cell used in next generation solar cells", *Journal of Semiconductors*, vol. 35, no. 9, pp. 094010, 2014.
- [20] A. B. Cornfeld, P. Patel, J. Spann, D. Aiken, and J. McCarty, "Evolution of a 2.05 eV AlGaInP top sub-cell for 5 and 6J-IMM applications", in *38th IEEE Photovoltaic Specialist Conference, 2012*, pp. 002788-002791.
- [21] L. C. Su, I. H. Ho, and G. B. Stringfellow, "Effects of substrate misorientation and growth rate on ordering in GaInP", *Journal of Applied Physics*, vol. 75, no. 10, pp. 5135-5141, 1994.
- [22] *Spontaneous ordering in semiconductor alloys*. A. Mascarenhas, ed., Eds., (Kluwer Academic/Plenum Publishers, 2002).
- [23] R. M. France, I. Garcia, W. E. McMahon, A. G. Norman, J. Simon, J. F. Geisz, D. J. Friedman, and M. J. Romero, "Lattice-mismatched 0.7-eV GaInAs solar cells grown on GaAs using GaInP compositionally graded buffers", *IEEE Journal of Photovoltaics*, vol. 4, no. 1, pp. 190-195, 2014.
- [24] A. L. Fahrenbruch and R. H. Bube, *Fundamentals of solar cells photovoltaic solar energy conversion* (Academic Press, New York, 1983).
- [25] M. A. Steiner, I. García, D. J. Friedman, A. Duda, W. J. Olavarria, M. Young, D. Kuciauskas, and S. Kurtz, "Effects of internal luminescence and internal optics on Voc and Jsc of III-V solar cells", *IEEE Journal of Photovoltaics*, vol. 3, no. 4, 2013.
- [26] H. J. Hovel, *Solar cells*. R. K. Willardson and A. C. Beer, Eds., Semiconductors and semimetals (Academic Press, New York, 1975), vol. 11.